

Exploring supramolecular interactions between inorganic tetrachlorometallate and organic pyridinium dication: Synthesis, characterization and structural investigations

Kamal Kumar Bisht, Amal Cherian Kathalikkattil, Suresh Eringathodi *

Analytical Science Discipline, Central Salt & Marine Chemicals Research Institute, Council of Scientific and Industrial Research (CSIR), GB Marg, Bhavnagar 364 002, Gujarat, India

ARTICLE INFO

Article history:

Received 2 November 2011

Received in revised form 14 January 2012

Accepted 17 January 2012

Available online 25 January 2012

Keywords:

Supramolecular chemistry

Tetrachlorometallate

Hydrogen bonding

Pyridinium dication

X-ray crystallography

Organic–inorganic hybrid

ABSTRACT

The crystal structures of three isostructural salts **2**, **3** and **4** consisting of dication (α,α' -*p*-xylylene-*N,N'*-bis(3-hydroxymethylpyridinium) (L^{2+}), and tetrachlorometallates, $[MCl_4]^{2-}$ ($M = Co(II), Zn(II)$ and $Cu(II)$ in **2**, **3** and **4** respectively) have been reported. Synthesized salts are well characterized by various physico-chemical techniques such as CHN analysis, IR, TGA, DSC, NMR, PXRD and single crystal X-ray diffraction. The crystal lattice of complex **2** is constructed from two types of interactions viz., C–H···Cl and O–H···Cl H-bonding between the pyridinium dication and the complex anions $[CoCl_4]^{2-}$, whereas only C–H···Cl interaction was found to play major role in stabilizing the structures of organic inorganic hybrid complexes **3** and **4**. The hierarchy of intermolecular interactions present in solid state, factors controlling the adopted structures of these compounds and their thermal stability are discussed in detail by using various analytical techniques including single crystal X-ray.

© 2012 Elsevier B.V. All rights reserved.

1. Introduction

Crystal engineering is a rapidly growing area of research, which mainly try to establish the command over the preparation of crystalline solid materials with detailed understanding of intermolecular attractions in the solid state, and the use of this understanding in the design of new solids with specific structural topologies and applications. Wide range of possible molecular and supramolecular interactions has been utilized for the construction of multidimensional networks [1]. Hydrogen bonding, van der Waals forces and $\pi \cdots \pi$ stacking etc. weak molecular interactions chiefly direct the design of organic solid state [2–5] whereas coordinative covalent bonds are equally important in the design and construction of coordination polymers [6–9]. Salts consisting of organic cations frequently exhibit ionic liquid behavior, and the properties associated with them such as magnetic, optical, electrical and catalytic activity can be tuned with subtle structural changes on cationic and/or anionic moieties [10,11]. In order to design a salt with preferred properties it is needful to precisely develop structure–property relationships for such compound [12,13]. This is one of the major reasons for the popularity of organic salts among crystal engineers and solid state researchers. Salts of organic cations with

tetrahalometallates have gained enormous attention due to the ease of designer synthesis, and applications [14–20]. In the case of *N*-alkylpyridinium tetrahalometallates, most of the studies focused on their liquid crystal or ionic liquid behavior [14–16]. However, synthesis and crystallographic studies on dicationic pyridinium salts involving tetrahalometallate are relatively few in the literature [21–23]. Interestingly, several reports including crystallographic studies in which tetrahalometallate (II) dianion combined with two organic cations possessing unit formal positive charge, is available in literature [24–29]. Self-assembly process of such hybrid materials in solid state arises due to the variety of interactions which include, ionic interactions, hydrogen bonding within the organic moiety, hydrogen bonding between organic and inorganic components, halogen bonding and van der Waals interactions [17]. Some pioneering work in this field by utilizing supramolecular synthon approach and exploiting the directional properties of hydrogen bonding interactions among tetrahalometallates and various organic cations has been carried out by Orpen and Brammer groups. In fact, Orpen, Brammer and their co-workers have utilized supramolecular synthons based on N–H···Cl hydrogen-bonds in the construction of organic–inorganic hybrid solids comprising organic cations with linear connectivity [18–20]. The effect of functional groups such as pendent hydroxyl groups on the physical properties of organic salts has been reported by several groups; Armstrong et al., have demonstrated the effect of symmetry on the melting points and other physical

* Corresponding author.

E-mail addresses: esuresh@csmcric.org, sureshe123@rediffmail.com (S. Eringathodi).

properties of dicationic ionic liquids [30]. On the other hand, there are very few reports demonstrating the role of O–H···Cl–M interactions in structural assemblies of organic tetrachlorometalate salts [31–33]. We have initiated some work in the area of self-assembled hybrid organic/inorganic materials as either multi-dimensional coordination polymers or layered structures via coordinate covalent bond or in conjunction with weak supramolecular hydrogen bonding interaction [9,34–38].

Herein we report the structural characterization of three tetrachlorometalate salts of organic pyridinium dication α,α' -*p*-xylylene-*N,N'*-bis(3-hydroxymethylpyridinium) (L^{2+}) and discuss various intermolecular interaction particularly the O–H···Cl–M, C–H···Cl interactions in the absence of charge assisted $N^+–H···Cl–M$ or $N–H···Cl–M$ interactions. In addition to the hydrogen bonding between the metal halide with the organic dication, conformational flexibility around the methylene carbon bridging the central phenyl and pyridine rings in the symmetrically disposed dication and the π -stacking between the six membered ring as well as C–H··· π interaction also partake in the supramolecular arrangement between the pyridinium salts of perchlorometallates in the present investigation. The effect of employed metal and geometry of tetrachlorometalate on the thermal stability is also accounted.

2. Experimental

2.1. Materials

Pyridine-3-methanol and α,α' -dichloro-*p*-xylene were purchased from Sigma–Aldrich. Metal chloride salts and organic solvents were obtained from SD Fine Chemicals, India. Double distilled water and methanol were used as solvents for the syntheses of the complexes. All the reagents and solvents were used as received without further purification.

2.2. Physical measurements

CHNS analyses were done using a Perkin–Elmer 2400 CHNS/O analyzer. IR spectra were recorded using KBr pellets on a Perkin–Elmer GX FTIR spectrometer. For each IR spectra 10 scans were recorded at 4 cm^{-1} resolution. ^1H and ^{13}C NMR spectra for the compounds were recorded on Bruker AX 500 spectrometer (500 MHz) at temperature 25 °C. NMR Spectra was calibrated with respect to internal reference TMS. Melting points of finely powdered samples were obtained using a Mettler Toledo FP62 instrument and are uncorrected. TGA analyses were carried out using Mettler Toledo Star SW 8.10. DSC analyses were carried out using Mettler Toledo DSC822e. Mass spectra were recorded on a Q-TOF Micro™ LC–MS instrument. Solution phase and solid state UV–Vis spectra were recorded using a Shimadzu UV-3101PC spectrophotometer. X-ray powder diffraction data were collected using a Philips X-Pert MPD system with Cu $K\alpha$ radiation. Single crystal structures were determined using a BRUKER SMART APEX (CCD) diffractometer.

2.3. Synthesis of α,α' -*p*-xylylene-*N,N'*-bis(3-hydroxymethylpyridinium) dichloride: $L^{2+}\cdot 2\text{Cl}^-$ (**1**)

$L^{2+}\cdot 2\text{Cl}^-$ has been synthesized by following a procedure reported by us recently [38]. To a solution of α,α' -dichloro-*p*-xylene (175 mg, 1 mmol) in 20 mL acetonitrile, pyridine-3-methanol (240 mg, 2.2 mmol) dissolved in 15 mL acetonitrile was added slowly. The reaction mixture was set to reflux for 6 h when the product formed as a white precipitate. The reaction mass was filtered, washed with 5 mL acetonitrile and dried in the air. The pure $L^{2+}\cdot 2\text{Cl}^-$ (**1**) obtained in good yield (294 mg, 74%) was soluble in water and organic

solvents such as methanol, ethanol, dimethylformamide and dimethyl sulfoxide. Similar solubility trend was observed for **2–4**.

Melting point: 182–184 °C; Elemental Anal. Calc. for $L^{2+}\cdot 2\text{Cl}^-$: C, 56.08; H, 5.88; N, 6.54; O, 14.94%. Found: C, 55.97; H, 5.92; N, 6.51; O, 15.03%. *m/z*: 357.20 ($[L^{2+}\text{Cl}^-]$, calculated 357.13), 321.19 ($[L^{2+}-\text{H}^+]$, calculated 321.16). IR (KBr): 3405s, 3190s, 3023s, 2940m, 1625s, 1500s, 1467m, 1443m, 1430s, 1371w, 1224s, 1191m, 1140s, 1057s, 994m, 928w, 863w, 816w, 768s, 745m. ^1H NMR (MeOD) δ : 9.07 (2H, s), 9.01 (2H, d, $J = 5.94$ Hz), 8.56 (2H, d, $J = 7.99$ Hz), 8.09 (2H, dd, $J = 5.94$ Hz, $J = 7.99$ Hz), 7.64 (4H, s), 5.92 (4H, s), 4.83 (4H, s); 13 C NMR (MeOD) δ : 143.9, 143.1, 142.6, 141.7, 134.6, 129.3, 127.3, 63.1, 59.2.

2.4. Synthesis of α,α' -*p*-xylylene-*N,N'*-bis(3-hydroxymethylpyridinium) tetrachlorocobaltate (II) monohydrate: $L^{2+}\cdot [\text{CoCl}_4]^{2-}\cdot \text{H}_2\text{O}$ (**2**)

A mixture of the **1** (42 mg, 0.1 mmol) and $\text{CoCl}_2\cdot 6\text{H}_2\text{O}$ (24 mg, 0.1 mmol), dissolved in 14 mL water–methanol (1:1) mixture was heated at 85 °C with continuous stirring for 2 h. The pink colored solution obtained was filtered and filtrate was dried using a rotary evaporator to obtain Complex **2** as a blue crystalline powder. Blue colored single crystals suitable for crystallographic studies were grown by recrystallization from methanol in a period of 2 weeks. Yield 50 mg (92%). Melting point: 110–112 °C; Elemental Anal. Calc. for **2**: C, 44.39; H, 4.47; N, 5.18; O, 8.87%. Found: C, 44.36; H, 4.54; N, 5.16; O, 8.93%. IR (KBr): 3393br, 3065m, 2940w, 2361m, 1626s, 1500s, 1472s, 1444m, 1293w, 1226m, 1143m, 1051s, 913w, 746m, 601w, 480w. ^1H NMR (MeOD) δ : 9.03 (2H, s), 8.96 (2H, d, $J = 5.63$ Hz), 8.54 (2H, d, $J = 7.58$ Hz), 8.07 (2H, dd, $J = 5.63$ Hz, $J = 7.58$ Hz), 7.61 (4H, s), 5.88 (4H, s), 4.84 (4H, s).

2.5. Synthesis of α,α' -*p*-xylylene-*N,N'*-bis(3-hydroxymethylpyridinium) tetrachlorozincate (II) monohydrate $L^{2+}\cdot [\text{ZnCl}_4]^{2-}\cdot \text{H}_2\text{O}$ (**3**)

A mixture of the **1** (42 mg, 0.1 mmol) and $\text{ZnCl}_2\cdot 6\text{H}_2\text{O}$ (25 mg, 0.1 mmol), dissolved in 14 mL water–methanol (1:1) mixture was heated at 85 °C with continuous stirring for 2 h. The pink colored solution obtained was filtered and filtrate was dried using a rotary evaporator to obtain Complex **3** as a white crystalline powder. Transparent single crystals suitable for crystallographic studies were grown by recrystallization from methanol in a period of 2 weeks. Yield 52 mg (95%). Melting point: 107–109 °C; Elemental Anal. Calc. for **3**: C, 43.87; H, 4.42; N, 5.12; O, 8.76%. Found: C, 43.82; H, 4.49; N, 5.08; O, 8.83%. IR (KBr): 3395br, 3069m, 2942w, 2362m, 1626s, 1500s, 1473s, 1446m, 1292w, 1228m, 1144m, 1053s, 912w, 745m, 602w, 485w. ^1H NMR (MeOD) δ : 9.03 (2H, s), 8.96 (2H, d, $J = 5.15$ Hz), 8.55 (2H, d, $J = 7.74$ Hz), 8.08 (2H, dd, $J = 5.15$ Hz, $J = 7.74$ Hz), 7.62 (4H, s), 5.89 (4H, s), 4.85 (4H, s).

2.6. Synthesis of α,α' -*p*-xylylene-*N,N'*-bis(3-hydroxymethylpyridinium) tetrachlorocuprate (II) monohydrate $L^{2+}\cdot [\text{CuCl}_4]^{2-}\cdot \text{H}_2\text{O}$ (**4**)

A mixture of the **1** (42 mg, 0.1 mmol) and $\text{CuCl}_2\cdot 6\text{H}_2\text{O}$ (24 mg, 0.1 mmol), dissolved in 14 mL water–methanol (1:1) mixture was heated at 85 °C with continuous stirring for 2 h. The pink colored solution obtained was filtered and filtrate was dried using a rotary evaporator to obtain Complex **4** as an orange–yellow colored crystalline powder. Bright yellow colored single crystals suitable for crystallographic studies were grown by recrystallization from methanol in a period of 3 weeks. Yield 50 mg (91%). Melting point: 95–97 °C; Elemental Anal. Calc. for **4**: C, 44.01; H, 4.43; N, 5.13; O, 8.79%. Found: C, 43.87; H, 4.52; N, 5.07; O, 8.84%. IR (KBr): 3400br, 3060m, 2948w, 2361m, 1624s, 1499s, 1470s, 1423m, 1291w,

Table 1
Crystal data and refinement parameters for Compound **2**, **3** and **4**.

Identification code	Compound 2	Compound 3	Compound 4
Chemical formula	C ₂₀ H ₂₂ Cl ₄ Co ₁ N ₂ O ₃	C ₂₀ H ₂₂ Cl ₄ Zn ₁ N ₂ O ₃	C ₂₀ H ₂₂ Cl ₄ Cu ₁ N ₂ O ₂
Formula weight	539.13	545.57	527.74
Crystal color	Blue	Colorless	Yellow
Crystal Size (mm)	0.37 × 0.33 × 0.11	0.47 × 0.28 × 0.14	0.21 × 0.15 × 0.05
Temperature (K)	110 (2)	110 (2)	110 (2)
Crystal system	Triclinic	Triclinic	Triclinic
Space group	<i>P</i> -1	<i>P</i> -1	<i>P</i> -1
<i>a</i> (Å)	8.1498(8)	8.1684(11)	8.0770(14)
<i>b</i> (Å)	8.5690(8)	8.6173(12)	8.6476(15)
<i>c</i> (Å)	16.9722(16)	17.170(2)	17.209(3)
α (°)	97.460(2)	97.796(2)	99.131(3)
β (°)	93.936(2)	93.831(2)	101.853(3)
γ (°)	101.587(2)	102.295(2)	98.832(3)
<i>Z</i>	2	2	2
<i>V</i> (Å ³)	1145.79(19)	1164.2(3)	1139.7(3)
Density (Mg m ⁻³)	1.563	1.556	1.538
Absorption coefficient (mm ⁻¹)	1.240	1.538	1.446
<i>F</i> (000)	550	556	538
Reflections collected	6921	8195	7495
Independent reflections	5061	4048	3557
<i>R</i> _(int)	0.0190	0.0372	0.0379
Number of parameters	264	273	273
<i>S</i> (Goodness of fit) on <i>F</i> ²	1.099	1.040	1.188
Final <i>R</i> ₁ / <i>wR</i> ₂ (<i>I</i> > 2 σ (<i>I</i>))	0.0671/0.1609	0.0723/0.2034	0.0967/0.2111
Weighted <i>R</i> ₁ / <i>wR</i> ₂ (all data)	0.0735/0.1652	0.0844/0.2146	0.1154/0.2207
CCDC number	831,072	831,073	831,074

1225m, 1142m, 1054s, 912w, 745m, 601w, 486w. ¹H NMR (MeOD) δ : 9.09 (2H), 9.02 (2H), 8.58 (2H), 8.12 (2H), 7.68 (4H), 5.94 (4H), 4.89 (4H).

2.7. X-ray crystallography

Summary of crystallographic data and details of data collection for all the three compounds are given in Table 1. In case of all the three compounds, single crystals of suitable size were mounted on the tip of a glass fiber and the intensity data were collected using MoK α ($\lambda = 0.71073$ Å) radiation on a Bruker SMART APEX diffractometer equipped with CCD area detector at 100 K.

The data integration and reduction were carried out with SAINT [39] software. An empirical absorption correction was applied to the collected reflections with SADABS [40]. The structures were solved by direct methods using SHELXTL [41] and were refined on *F*² by the full-matrix least-squares technique using the SHELXL-97 [42] program package. The lattice water molecule present in the case of Complex **4** was highly disordered and their contribution to the diffraction pattern has been removed using the SQUEEZE subroutine as implemented in PLATON [43]. Refinement of **4** using the modified reflection data set apparently improved the *R*-factor. All non-hydrogen atoms were refined anisotropically till convergence is reached. Hydrogen atoms attached to the dication moieties are stereochemically fixed in all the complexes. However,

hydrogen atoms could not be located from the difference Fourier map for lattice water molecules.

3. Results and discussion

3.1. IR, LCMS and PXRD analysis

The IR spectra of pyridinium dicationic salt **1** consists of a weak band around 912 cm⁻¹ which can be attributed to the C–N stretching band of quarternary pyridinium entity, suggesting the formation of adduct between α,α' -dichloro-*p*-xylene and pyridine-3-methanol. However, the formation of symmetric dicationic salt is confirmed by the LCMS and NMR techniques. Methanol solution **1** was subjected to time of flight mass spectrometry (TOF-MS). The mass spectra clearly shows *m/z* peaks corresponding to [L²⁺·Cl⁻] at 357.20 (calculated value 357.13), and low intensity peak for [L²⁺–H⁺] at 321.19 (calculated value 321.16). The base peak at *m/z* 161.09 and second most intense peak at *m/z* 230.10 represent two unsymmetrical but complementary molecular fragments of **1** resulted by cleaving of one of the arene methylene bond and equal distribution of two chloride ions. The IR spectra of **1–4** encompass two broad bands around 3550 and 3190 cm⁻¹ suggesting the presence of lattice water molecules in these compounds in addition to the alcohol functionality. O–H stretching bands of the alcoholic group for **1–4** is observed at 3190, 3393, 3395, 3400 cm⁻¹ respectively. The aromatic C–H stretching frequencies for tetrahalometallates **2–4** appeared at 3065, 3069 and 3060 cm⁻¹ respectively. The quantitative differences among these three values suggest the involvement of hydrogen atoms attached to aromatic rings in hydrogen bonding interactions. The aromatic C–H deformation bands for **1–4** appeared at 1467, 1472, 1473, 1470 cm⁻¹ respectively. Medium intensity signals around 1625, 1500 and 1446 cm⁻¹ for all the compounds **1–4** are attributable to the aromatic unsaturated C–C bonds. Medium intensity signals at 1430, 1444, 1426 and 1423 cm⁻¹ can be attributed to the deformation mode of hydrogen bonded methylene groups in the case of **1–4**. The presence of sharp peaks around 770 cm⁻¹ in all the compounds **1–4** can be attributed to the methylene rock mode. Weak bands around 480 and 420 cm⁻¹ in infrared profiles of **2–4** can be attributed to the metal chloride linkage of tetrachlorometallate anions. In an attempt to confirm the homogeneity of the synthesized materials, we have analyzed the XRPD pattern of compounds **2–4** and correlated the results with the powder pattern obtained from the single crystal XRD data simulation. The experimental XRPD patterns corroborate well with the corresponding powder patterns simulated from single crystal data, indicating the phase purity of bulk products. Phase purity was further confirmed by comparing the unit cell parameters obtained from single crystal XRD data and the same calculated from XRPD data. Details of unit cell parameter determination, XRPD profiles and IR spectra for **2–4** and LCMS for **1** are given in Supplementary data information.

3.2. NMR analysis

¹³C NMR spectra of **1** comprise of nine well distinguished resonance signals in the chemical shift range of 143.9–59.2 ppm. These signals are attributable to the centrosymmetric structure of the dication which is further evident by ¹H NMR spectroscopy. The ¹³C NMR spectra for **1** and ¹H NMR spectra for **1–4** are given in Supplementary information with the structural assignment of observed signals. The proton shifts for tetrachlorometallate salts **2–4** were consistent with that of **1** indicating same dication in all of the reported compounds **1–4**. However, the observed differences in the chemical shifts and coupling constants can be attributed to the different metal ions, different anionic geometry and difference

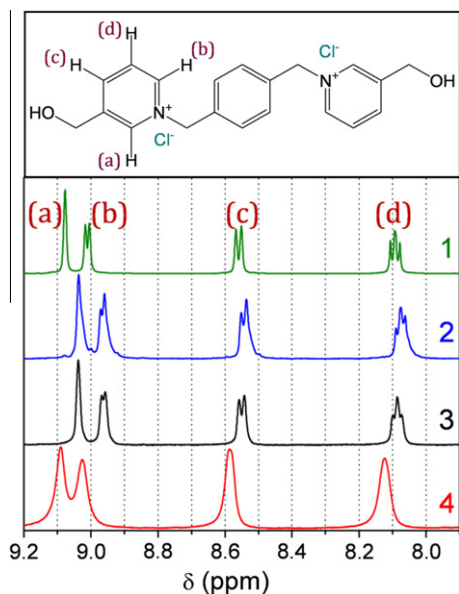


Fig. 1. A segment of room temperature ^1H NMR spectra exhibiting the chemical shifts and coupling patterns for pyridinium protons in salts **1–4** in $\text{MeOD}-d$ solvent. Lowercase alphabets in parentheses represent the magnetically non-equivalent pyridinium protons of dication as represented in inset.

in hydrogen bonding contacts between the cation and anion in solution phase. Fig. 1 presents a comparison of chemical shifts for pyridinium protons in **1–4** and reveals slight shielding for the same in **2–4** with respect to **1**. The NMR spectra of paramagnetic substances contain valuable information, but the scattered chemical shifts and fast nuclear relaxation (broad lines) renders them difficult to interpret [44–46]. In an attempt to deal with the paramagnetic Co^{2+} (d^7 system) system we have recorded solution state proton NMR spectra for **2** in different deuterated solvents viz., D_2O , methanol- d , $\text{DMSO}-d^6$ and $\text{DMF}-d^7$. Except in $\text{DMF}-d^7$, the occurrence of clean NMR spectra for **2** can be attributed to the highly symmetric T_d geometry for $[\text{CoCl}_4]^{2-}$ ion [14c]. Dimethyl formamide being highly polar and good coordinating solvent is expected to interact with $[\text{CoCl}_4]^{2-}$ persuading in strong distortions from T_d symmetry, resulting the clumsiness of proton NMR spectra in $\text{DMF}-d^7$. The effect of paramagnetic nature of Co^{2+} (d^7) and Cu^{2+} (d^9) systems can be observed in the coupling behavior of protons as depicted in Fig. 1. The signals for pyridinium protons b, c and d become considerably unsymmetrical for **2** (Co^{2+} , d^7 system) and interestingly, peak broadening for signals resulted in single bands in the case of **4** (Cu^{2+} , d^9 system) may be due to the highly distorted tetrahedral geometry adopted by the $[\text{CuCl}_4]^{2-}$ as observed in X-ray data.

3.3. Thermal analyses

All the tetrachlorometallate salts are air-stable and retain their crystalline integrity under ambient conditions. Thermogravimetric analysis (TGA) and differential scanning calorimetry (DSC) experiments in nitrogen atmosphere were carried out in order to determine the thermal stability, dehydration and decomposition of compounds **2–4** and the results are presented in Fig. 2.

The thermograms for **2** and **3** apparently suggest the higher thermal stability of tetrachlorocobaltate and tetrachlorozincate salts. Both **2** and **3** loss lattice water (observed (calculated) weight loss for **2** and **3** 4.21 (3.33) and 4.1(3.29)% for **2** and **3** respectively) in 55–105 °C temperature range with exclusion points nearing 79 and 78 °C respectively. The determined melting points of **2** and **3**

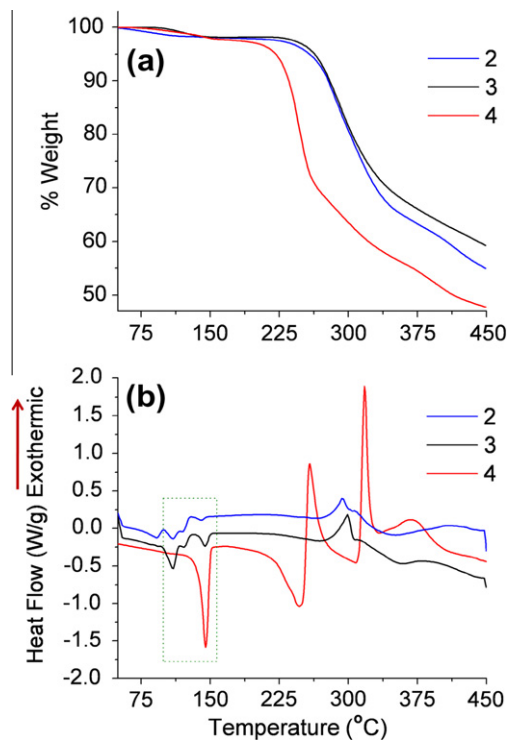


Fig. 2. TGA and DSC plots for pyridinium salts **2–4** in temperature range 50–450 °C. The endothermic signals in DSC near melting points of **2–4** are surrounded by a rectangle. (All TGA and DSC plots were obtained at a scan rate of 10 °C min^{-1} ; (a) and (b) share the identical x-axis.)

reside in the range 106.5–108.5 and 103–105 °C respectively. TGA profiles suggest excellent thermal stability of these compounds as higher as 100° above their respective melting points. A two step decomposition is observed in the temperature range 220–340 °C for both **2** and **3** with 35% weight loss of their initial weight followed by the slow decomposition of the residual materials with increase in temperature. Close resemblance of DSC Plots for **2** and **3** indicate three unknown phase changes immediate after the expulsion of lattice water molecules around 110, 120.5 and 140 °C for **2** and 108.5, 122 and 144.5 °C for **3** respectively. Tetrachlorocuprate salt **4** exhibits weight loss process in the temperature ranges 85–145 and 195–260 °C. A weight loss of 3.1% near about 95 °C can be attributed to loss of lattice water molecule (calculated weight loss 3.32%). The absence of intense heat flow signal near 95 °C in the DSC plot for **4** suggests weak interactions between the guest water molecules and the organic salt. The second decay process recorded on TGA comprises of 31.48% mass loss at 235 °C indicating the commencement of decomposition of the compound which follows the same trend as observed in the case of **2** and **3**. The determined melting point for **4** is 140–142 °C. The decomposition of compound **4** maps out intense endothermic minima at 204.5 °C whereas preceding shoulder nearby 140 °C represents melting phenomenon. The correlations among melting points, thermograms and DSC plots for all three compounds **2–4** suggest that the tetrachlorometallates **2–4** are fairly stable salts and their thermal decomposition realize after melting. Moreover, complexes **2** and **3** exhibited excellent thermal stability even up to the temperatures as high as 100° above their melting points.

3.4. UV–VIS absorption study

UV–vis absorption experiments were performed at room temperature for **1–4** in 10^{-4} M methanolic solutions as well as in solid state. The solution phase absorption spectra presented in Fig. 3a

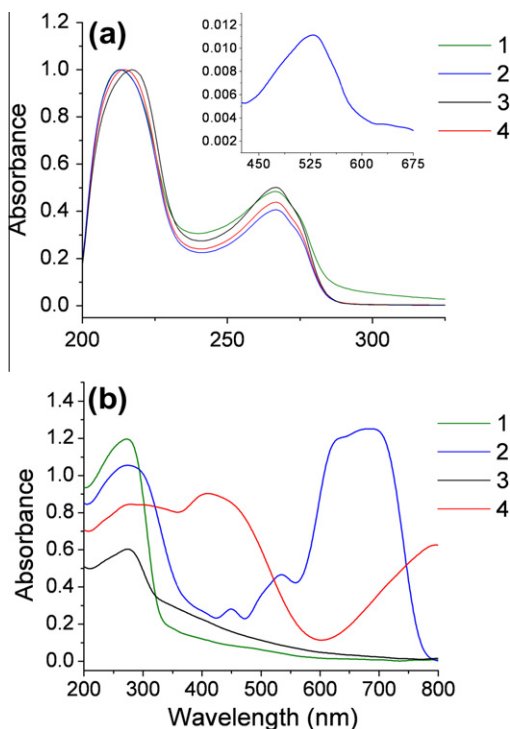


Fig. 3. (a) Absorption spectra for **1–4** in 10^{-4} M methanolic solutions recorded at room temperature; *d–d* band observed for 10^{-3} M methanolic solution of cobalt(II) compound **2** is presented in inset. (b) Solid state uv–vis absorption spectra of **1–4** recorded at room temperature.

shows that the compound **1** absorbs strongly at 212 nm and 267 nm, however, methanolic solutions of **2–4** follow similar trend. Compounds **2**, **3** and **4** exhibited a weak bathochromic shift as compared to 212 nm signal of **1**, and absorb at 213, 217 and 214 nm respectively. The *d–d* transition for **2** appears at 530 nm whereas the same transition for **4** could not be recorded at studied dilution. Solid state absorption spectra are recorded with unpolarized source and are presented in Fig. 3b. Salt **1** intensely absorbs in the uv region 272 nm at room temperature. The tetrachlorometallate salts **2–4** also absorb in the same region at 274, 274 and 279 nm respectively with considerable decrease in absorbance intensity. Salt **2**, that contain $[\text{CoCl}_4]^{2-}$ showed absorption bands at 449 and 535 nm ($22,271$ and $18,691 \text{ cm}^{-1}$) for ligand field transitions and a broad band around 685 nm ($14,598 \text{ cm}^{-1}$) that may envelop *d–d* (${}^4A_2 \rightarrow {}^4T_2$, ${}^4A_2 \rightarrow {}^4T_1(F)$, ${}^4A_2 \rightarrow {}^4T_1(P)$) transitions. Compound **3** exhibited feebly distinct ligand field transitions in 345–455 nm range. This moderate intensity band appears as a shoulder to the 274 nm band observed for cation L^{2+} . Compound **4**, which contains the D_{2d} distorted tetrahedral $[\text{CuCl}_4]^{2-}$ complex exhibited LMCT band around 410 nm ($24,390 \text{ cm}^{-1}$). The broad overlapping bands in lower energy region that extends to the near-IR region envelop *d–d* (${}^2B_2 \rightarrow {}^2A_1$, ${}^2B_2 \rightarrow {}^2B_1$, ${}^2B_2 \rightarrow {}^2E$) transitions. The spectral features of **4** with average *trans* angle $\sim 135^\circ$ are in accordance with previously reported tetrachlorocuprate salts [47–49]. A comparative overview of Fig. 3 reflects the considerable differences between solution and solid state spectra for each of **1–4** and points out that choice of metal center and coordination driven slight variations in crystal packing may considerably affect the absorption properties of isostructural salts.

3.5. Crystal and molecular structures of $L^{2+} \cdot [\text{CoCl}_4]^{2-} \cdot \text{H}_2\text{O}$; **2**, $L^{2+} \cdot [\text{ZnCl}_4]^{2-} \cdot \text{H}_2\text{O}$; **3** and $L^{2+} \cdot [\text{CuCl}_4]^{2-} \cdot \text{H}_2\text{O}$; **4**

ORTEP diagram ($[\text{MCl}_4]^{2-}$ with one pyridinium dication) and crystallographic data for all the three complexes are given in

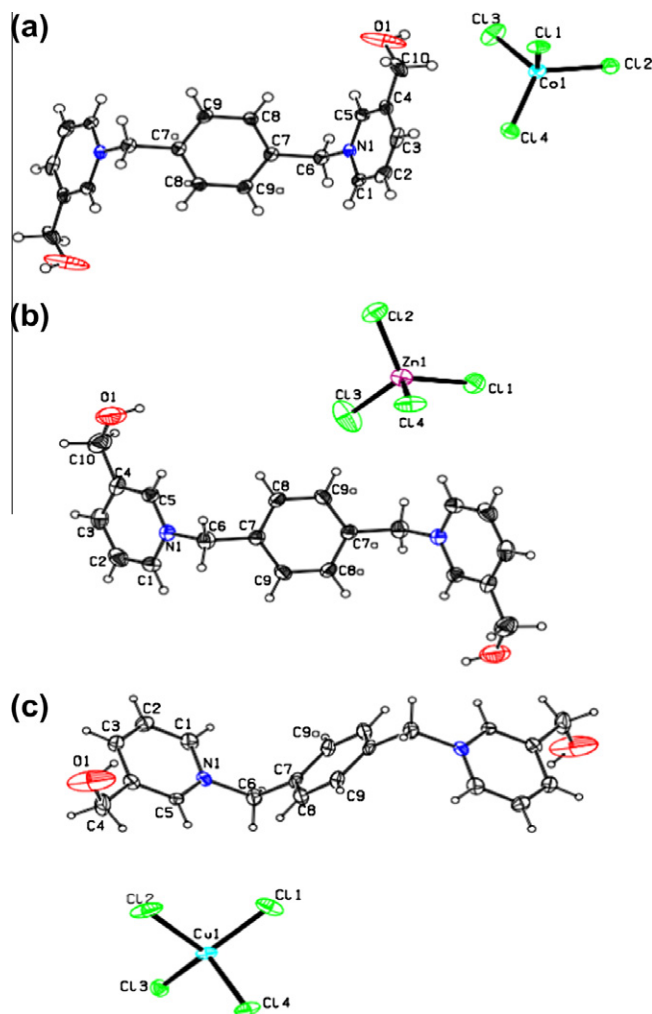


Fig. 4. ORTEP diagram of tetrachlorometallate salts **2–4** (40% probability factor for the thermal ellipsoids; lattice water molecules are omitted for clarity).

Fig. 4 and Table 1 respectively. It is worthy to mention that the three crystal structures possess almost the same unit cell parameters. All the three complexes are isostructural and crystallized in triclinic space group *P-1* with slight variation in the crystallographic parameters viz., cell dimensions and cell volume. The variation in crystal parameters may be attributed to the existence of different metal ions, flexibility of the dication and difference in mode of intermolecular interactions in these complexes. The asymmetric unit of all the three complexes consists of one $[\text{MCl}_4]^{2-}$ anion occupying the general position and two centrosymmetric half cations with the center of inversion located at the middle of the phenyl ring along with one water molecule as solvent of crystallization.

The crystal structures of all the three complexes consist of isolated pyridinium dications and distorted tetrahedral $[\text{MCl}_4]^{2-}$ (where M = Co(II), Zn(II) and Cu(II)) anions along with one water molecule as solvent of crystallization. The anion of complex **2** and **3** i.e. $[\text{CoCl}_4]^{2-}$ and $[\text{ZnCl}_4]^{2-}$ reveal a slightly distorted tetrahedral geometry with Cl–M–Cl angles in the range $105.26(5)$ – $114.81(5)^\circ$ and $104.75(8)$ – $113.81(7)^\circ$ respectively. In the case of **4**, $[\text{CuCl}_4]^{2-}$ exhibits a distinctive, highly distorted tetrahedral geometry in which the Cl–Cu–Cl is in the range of $98.93(15)$ – $138.11(13)^\circ$. The average value of the Cl–Cu–Cl *trans* angles is 135.64° , indicating the high distortion in the tetrahedral geometry that can be attributed to the Jahn–Teller effect of the Cu(II) and the packing arrangement imposed by the dication. In the case of Co

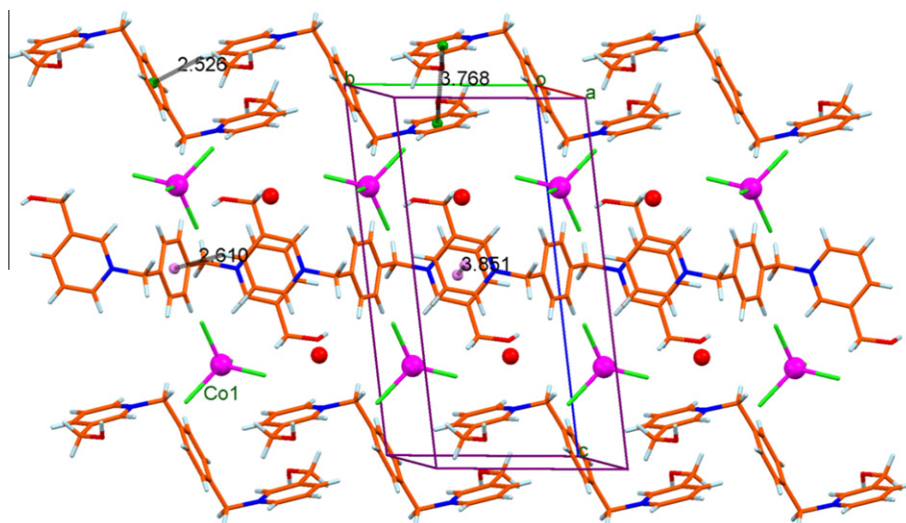


Fig. 5. Packing diagram of compound **2** viewed down *a*-axis showing stacking, C–H... π interaction between the layered dications and the orientation of the $[\text{MCl}_4]^{2-}$ anion and water molecules between the adjacent dicationic layers.

and Zn complexes the Cl–M–Cl are much closer to the ideal tetrahedral value (111.29° and 112.55° respectively). M–Cl distance range in compounds **2**, **3** and **4** are 2.2570(13)–2.2946(13), 2.2534(18)–2.282(2) and 2.226(3)–2.247(3) respectively. These bond distances as well as the bond angles cited for the tetrachlorometallate complexes are well within the range of the earlier reports [18–29]. Tetrahedral geometry is less distorted as expected for the d^7 and d^{10} tetrahedral ions in the cases **2** and **3** compared to d^9 system in the case of Cu complex **4**. In all the three salts, the dication adopts *anti* conformation. The pyridinium rings of symmetrically disposed dication in **2–4** are essentially planar and are parallel to each other. However, the tilt angle between the

central phenyl ring and the pyridine rings shows slight differences. The tilt angle between the phenyl ring and pyridyl rings in the centrosymmetric dication for **2–4** are 75.77° , 73.18° ; 75.78° , 72.23° ; 76.78° , 74.60° respectively.

In an attempt to understand the molecular interactions between the $[\text{MCl}_4]^{2-}$ anion and pyridinium dication we have analyzed the packing of the molecules and hydrogen bonding interactions in detail. Since the anions carry four potential hydrogen bond acceptors and range of apparent hydrogen bond donor sites is available with the organic dication, numerous ways in which the cations and anions might be arranged to give satisfactory hydrogen bonds are feasible. Furthermore flexibility of the

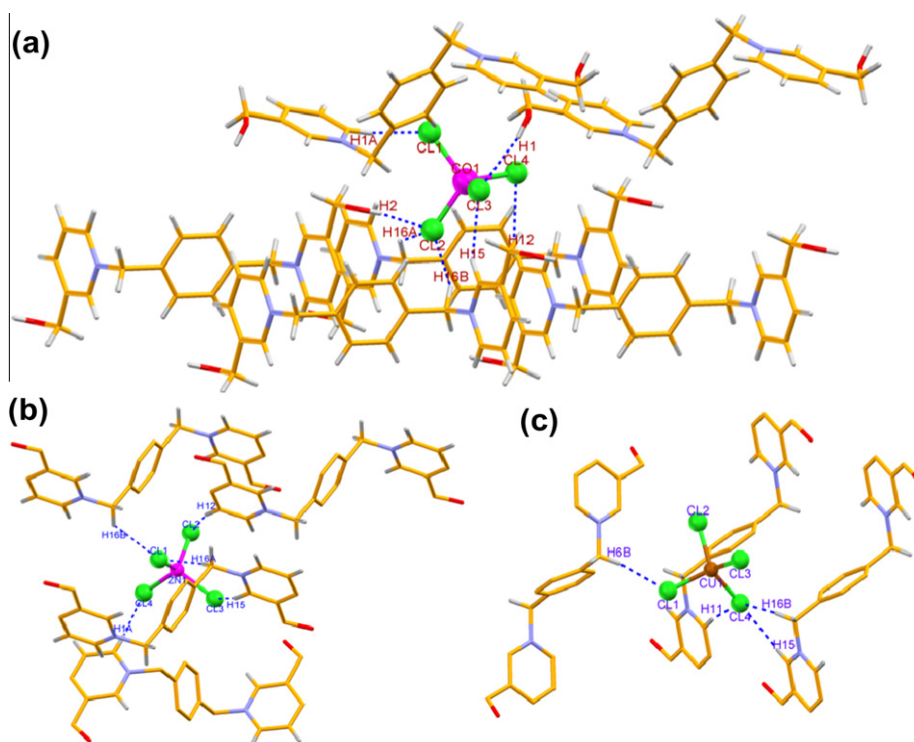


Fig. 6. Close up view of the hydrogen bonding interactions between $[\text{MCl}_4]^{2-}$ and L^{2+} in compounds **2–4**.

organic cation and stacking interactions among organic moieties also promote the weak molecular interaction in the formation of supramolecular network.

Packing diagram of the Co complex (**2**) as a representative of the isostructural organic salts **2–4** is viewed down *a*-axis is shown in Fig. 5. It depicts two different types of superimposed rows of pyridinium dications in **2**. There are two crystallographically distinct L^{2+} cations aligned along the *b*-axis in these isostructural compounds. Each centrosymmetric cation is associated with the same cation via intermolecular stacking resulting in the columns of alternate cationic layers (in plane and perpendicular) in their orientation (in *bc*-plane) with the stacking axis down *a*-axis (Fig. 5). Single row of $[MCl_4]^{2-}$ anions and the lattice water molecules are positioned between these two different dicationic layers and are held together through secondary C–H...Cl/O–H...Cl hydrogen bonding interactions. Stacking interactions between pyridinium rings can be seen along the *a*-direction and *b*-direction defining two different types of superimposed rows of pyridinium rings. Both the $\pi \cdots \pi$ interactions are reached through almost face-to-face alignment with inter-planar distances 3.56, 3.61 Å (and the centroid...centroid distance 3.76, 3.85 Å), and horizontal slippage of 1.23 and 1.35 Å for the Co complex. Similar trend is observed in the isostructural complexes **3** and **4**, with the face-to-face interplanar stacking distance of 3.58, 3.71 Å (centroid...centroid distance 3.84, 3.92 Å) and horizontal slippage of 1.41 and 1.28 Å for Zn salt and 3.73, 3.58 Å (centroid...centroid distance 4.07, 3.78 Å) with horizontal slippage of 1.63 and 1.22 Å for the copper complex generating layers of the dications. In addition to the above stacking interactions between the terminal pyridinium rings originated from the exclusive stacking of the symmetrically disposed dication present in the asymmetric unit from either side, alternate layers of pyridinium dications within the cationic layer is further stabilized by intermolecular C–H... π interaction as depicted in Fig. 5 along *b*-axis. Thus, the H3 from the terminal pyridinium ring of the L^{2+} is involved in C–H... π with the central phenyl ring of the adjacent molecule within the self assembled first dicationic layer and H13 of the terminal pyridinium ring of the L^{2+} is involved in C–H... π with the central phenyl ring with the adjacent molecule within the π stacked second dicationic layer. Same trend of C–H... π interaction is observed in all the three complexes with slight variations in the

C–H... π parameters (H3...Cg = 2.53 Å for **1**; 2.63 Å for **2** and 2.78 Å for **3**; C3...Cg = 3.402(5) Å for **1**; 3.481(6) Å for **2**; 3.625(10) Å for **3**; C3–H3...Cg = 157° for **1**; 152° for **2** and 151° for **3** for the first dicationic layer and H13...Cg = 2.61 Å for **1**; 2.70 Å for **2** and 2.57 Å for **3**; C13...Cg = 3.402(5) Å for **1**; 3.515(7) Å for **2** and 3.448(9) Å for **3**; C13–H13...Cg = 157° for **1**; 147° for **2** and 158° for **3** for the second dicationic layer).

Fig. 5, clearly depicts that alternating rows of $\pi \cdots \pi$ stacked pyridinium rings are separated by rows of $[MCl_4]^{2-}$ anions. Even though complex **2–4** are isostructural, crystal structure analysis showed that hydrogen bonding interaction between the organic dication and $[MCl_4]^{2-}$ anions are quite different. Close up view of the hydrogen bonding interaction in all the three organic salts are depicted in Fig. 6. In the case of Co salt (**2**), six dicationic moieties are involved in two O–H...Cl and five C–H...Cl contacts surrounding the $[MCl_4]^{2-}$ anion as depicted in Fig 6a. Thus, the H1, H2 alcoholic hydrogens from different dications are involved in O–H...Cl contact with Cl3 and Cl2 of the $[CoCl_4]^{2-}$ (H1...Cl3 = 3.425(7) Å; H2...Cl1 = 3.158(4) Å with O–H...Cl = 152° and 169° respectively). Further, Cl2 and Cl3 acts as acceptors and involved in C–H...Cl contacts with methylene hydrogens H16A, H16B and the cationic pyridine hydrogen H15 respectively. Cl1 and Cl4 are involved in only one C–H...Cl contact with H12 and H1A of the pyridine moiety. Thus, each $[CoCl_4]^{2-}$ anion is held in place between the alternate dicationic layers by five C–H...Cl and two O–H...Cl totaling seven secondary hydrogen bonding interactions. Hydroxyl groups (O1 and O2) of the dicationic moiety and lattice water molecule O3 acts as hydrogen bonding acceptors and involve in C–H...O interactions with hydrogen atoms of the pyridinium ring in stabilizing the organic salt in the crystal lattice. In the case of Complex **3** only four units of dication are surrounded by the $[ZnCl_4]^{2-}$ involving in only C–H...Cl hydrogen bonding interactions. Thus, Cl1 is involved in two CH...Cl contacts with the methylene hydrogens H16A and H16B of different dicationic moiety while Cl2, Cl3 and Cl4 are involved in one C–H...Cl contact each with H12, H15 and H1A from the pyridine moiety of the L^{2+} in clasp the $[ZnCl_4]^{2-}$. Unlike **1**, complex **2** is occupied by only five C–H...Cl contacts involving all four Cl of the anion, hence hydroxyl group has no role in holding the anionic moiety. However, Hydroxyl group involving O1 and the lattice water molecule O3 acts as acceptors

Table 2
Hydrogen bonding interactions in Compound **2**, **3** and **4**.

Compound	D–H...A	d(H...A) (Å)	d(D...A) (Å)	D–H...A (°)
Compound 2	O(1)–H(1)...Cl(3) ¹	2.68	3.425(7)	152
	C(15)–H(15)...Cl(3) ¹	2.73	3.594(5)	156
	C(16)–H(16A)...Cl(2) ²	2.81	3.482(5)	127
	C(16)–H(16B)...Cl(2) ¹	2.66	3.563(5)	155
	O(2)–H(2)...Cl(2) ³	2.35	3.158(4)	169
	C(1)–H(1A)...Cl(1) ⁴	2.57	3.489(4)	170
	C(12)–H(12)...Cl(4) ⁵	2.72	3.568(5)	151
	C(11)–H(11)...O(3) ⁵	2.32	3.216(8)	161
	Symmetry code: (1) <i>x, y, z</i> ; (2) $1 - x, -y, 1 - z$; (3) $x, 1 + y, z$; (4) $1 + x, 1 + y, z$; (5) $1 - x, 1 - y, 1 - z$			
Compound 3	C(16)–H(16A)...Cl(1) ¹	2.69	3.574(8)	152
	C(16)–H(16B)...Cl(1) ²	2.82	3.556(8)	133
	C(12)–H(12)...Cl(2) ³	2.78	3.632(7)	153
	C(15)–H(15)...Cl(3) ¹	2.66	3.507(6)	152
	C(1)–H(1A)...Cl(4) ⁴	2.59	3.518(6)	172
	C(2)–H(2A)...O(1) ⁵	2.59	3.500(9)	168
	C(11)–H(11)...O(3) ⁶	2.29	3.205(9)	167
	Symmetry code: (1) <i>x, y, z</i> ; (2) $1 - x, 2 - y, -z$; (3) $1 - x, 1 - y, -z$; (4) $2 - x, 2 - y, 1 - z$; (5) $1 + x, y, z$; (6) $x, y, -1 + z$			
Compound 4	C(6)–H(6B)...Cl(1) ¹	2.67	3.612(11)	163
	C(11)–H(11)...Cl(4) ²	2.61	3.534(9)	172
	C(15)–H(15)...Cl(4) ¹	2.75	3.624(8)	156
	C(16)–H(16B)...Cl(4) ¹	2.82	3.695(9)	151
	O(2)–H(2)...O(2) ³	2.56	3.323(9)	155
	C(12)–H(12)...O(2) ²	2.56	3.440(10)	158
	Symmetry code: (1) <i>x, y, z</i> ; (2) $1 + x, y, z$; (3) $1 - x, -y, -z$			

via inter/intramolecular C–H···O interaction with the pyridinium hydrogens H2A, H5 and H11 in stabilizing the solid state structure. For complex **4**, only three dicationic moieties are drawn in hydrogen bonding with $[\text{CuCl}_4]^{2-}$ via C–H···Cl interaction. Interestingly, for **1** and **2**, all the four chloride ions of $[\text{MCl}_4]^{2-}$ moiety are implicated as good hydrogen bond acceptors in C–H···Cl/O–H···Cl contacts; while in the case of Cu complex **4**, only two chlorides Cl1 and Cl4 are making contacts with three different dicationic moieties. Thus, Cl1 as an acceptor is making C–H···Cl H bonding with the methylene hydrogen H6B, while Cl4 is making three C–H···Cl hydrogen bonds from the other two dicationic moieties chipping in methylene hydrogen H16B and pyridinium hydrogen H15 of the same cation and pyridinium hydrogen H11 of another cationic moiety. Hydroxyl group involving O2 is making intermolecular O–H···O H-bonding with the same dication and acts as an acceptor in C–H···O interaction with H12 in the generation of supramolecular hydrogen bonded nets. Details of all these pertinent hydrogen bonding interaction mentioned above for all the three tetrachlorometallates and their symmetry codes are given in Table 2.

Even though all the three complexes crystallized in the same space group with almost identical cell dimensions and crystal packing, hydrogen bonding interactions between $[\text{MCl}_4]^{2-}$ moiety and dications is quite different. This can be attributed to the subtle changes in the tetrahedral geometry of $[\text{MCl}_4]^{2-}$ due to the variation in the central metal, flexibility of the dication around the methylene groups which all concomitantly control the closer approach of the organic moiety surrounding the tetrachlorometallate in making effective hydrogen bonding interactions.

4. Conclusion

Pyridinium dication L^{2+} was shown to form crystalline solids when included into the hybrid salts $\text{L}^{2+}[\text{MCl}_4]^{2-}$ (M = Co, Zn, and Cu) which has shown isomorphism in solid state structural analysis by X-ray diffraction. All tetrachlorometallate salts were well characterized by various physico-chemical techniques such as CHN, IR, NMR, PXRD and X-ray crystallography. The self-assembly in the solid state is governed mainly by directional H-bonding interactions, ionic interaction between the organic dication and the anionic perchlorometallate and the stacking, C–H··· π interaction of the symmetrically disposed dications. C–H···Cl/O–H···Cl interactions observed in these H-bonded inorganic organic hybrid material underline the significance of C–H···Cl interactions as an important structure directing feature. In addition to the above cited hydrogen bonding interaction of $[\text{MCl}_4]^{2-}$ with organic cations, conformational flexibility of the organic moiety and the presence of other weak interactions like stacking of the six membered rings and C–H··· π interaction contribute significantly in the layered hydrogen bonded supramolecular network in these isostructural compounds. We have shown the role and importance of secondary non-covalent interactions (such as H-bonding, dipolar, and van der Waals attractions) in the self-organization of molecular components towards designing new supramolecular solid materials. Comparative analysis of these metal salts with respect to their thermal stability and solid state absorption behavior is also reported. Efforts are in progress to ponder the diverse molecular interactions in the same pyridinium dications with various anions having different shapes and charge in generating solid state supramolecular assemblies using X-ray diffraction and their application in the area of ionic liquids.

Acknowledgements

The authors are gratefully acknowledge the CSIR, India (Grant No. NWP-0010) and Department of Science and Technology

(DST), New Delhi, India (Grant No. SR/S1/IC-37/2006) for financial support. K.K.B. and A.C.K. acknowledge CSIR (India) and DST for JRF and SRF, respectively. The authors are grateful to Dr. Pragnya Bhatt for PXRD data Mr. Vinod Kumar Agrawal for IR data, Mr. Hitesh Bhatt for NMR data, Mrs. Sheetal N. Patel for TGA data, Mr. Viral Vakani for microanalysis, Mr. Arun Das for LCMS and Dr. P. Paul for all-round analytical support.

Appendix A. Supplementary material

CCDC 831072, 831073 and 831074 contain the supplementary crystallographic data for complex **2–4** respectively. These data can be obtained free of charge via <http://www.ccdc.cam.ac.uk/contents/retrieving.html> or from the Cambridge Crystallographic Data Centre, 12 Union Road, Cambridge CB2 1EZ, UK; fax: (+44) 1223-336-033; or e-mail: deposit@ccdc.cam.ac.uk. Supplementary data associated with this article can be found, in the online version, at [doi:10.1016/j.molstruc.2012.01.023](https://doi.org/10.1016/j.molstruc.2012.01.023).

References

- [1] G.R. Desiraju, *Crystal Engineering, The Design of Organic Solids*, Elsevier, Amsterdam, 1989.
- [2] G.R. Desiraju, *Angew. Chem., Int. Ed. Engl.* 34 (1995) 2311–2327.
- [3] G.R. Desiraju, T. Steiner, *The Weak Hydrogen Bond*, Oxford University Press, Oxford, UK, 1999.
- [4] V.R. Pedireddi, *CrystEngComm* 4 (2002) 315–317.
- [5] D.C. Sherrington, K.A. Taskinen, *Chem. Soc. Rev.* 30 (2001) 83–93.
- [6] O.M. Yaghi, M. O’Keeffe, N.W. Ockwig, H.K. Chae, M. Eddaoudi, J. Kim, *Nature* 423 (2003) 705–714.
- [7] C. Férey, C. Mellot-Draznieks, C. Serre, F. Millange, J. Dutour, S. Surblé, I. Margiolaki, *Science* 309 (2005) 2040–2042.
- [8] C.J. Adams, M.F. Haddow, M. Lusi, A.G. Orpen, *PNAS* 107 (2010) 16033–16038.
- [9] A.C. Kathalikkattil, K.K. Bisht, N. Aliaga-Alcalde, E. Suresh, *Cryst. Growth Des.* 11 (2011) 1631–1641.
- [10] P. Wasserscheid, T. Welton, *Ionic Liquids in Synthesis*, second ed., Wiley-VCH, Weinheim, 2008.
- [11] S.A. Forsyth, U. Fröhlich, P. Goodrich, H.Q.N. Gunaratne, C. Hardacre, A. McKeown, K.R. Seddon, *New J. Chem.* 34 (2010) 723–731.
- [12] A.R. Katritzky, R. Jain, A. Lomaka, R. Petrukhin, M. Karelson, A.E. Visser, R.D. Rogers, *J. Chem. Inf. Comput. Sci.* 42 (2002) 225–231.
- [13] M. Hatano, T. Maki, K. Moriyama, M. Arinobe, K. Ishihara, *J. Am. Chem. Soc.* 130 (2008) 16858–16860.
- [14] F. Neve, A. Crispini, O. Francescangeli, *Inorg. Chem.* 39 (2000) 1187–1194.
- [15] F. Neve, O. Francescangeli, A. Crispini, *J. Charmant, Chem. Mater.* 13 (2001) 2032–2041.
- [16] K.F. Wang, F.F. Jian, R.R. Zhuang, H.L. Xiao, *Cryst. Growth Des.* 9 (2009) 3934–3940.
- [17] B.K. Saha, A. Nangia, M. Jaskólski, *CrystEngComm* 7 (2005) 355–358.
- [18] G.R. Lewis, A.G. Orpen, *Chem. Commun.* (1998) 1873–1874.
- [19] A. Angeloni, A.G. Orpen, *Chem. Commun.* (2001) 343–344.
- [20] J.C. Mareque Rivas, L. Brammer, *Inorg. Chem.* 37 (1998) 4756–4757.
- [21] J. Chang, W. Ho, I. Sun, Y. Chou, H. Hsieh, T. Wu, *Polyhedron* 30 (2011) 497–506.
- [22] A.L. Gillon, A.G. Orpen, J. Starbuck, X.M. Wang, Y. Rodríguez-Martín, C. Ruiz-Pérez, *Chem. Commun.* (1999) 2287–2288.
- [23] S.A. Bourne, L.J. Moitsheki, *Polyhedron* 27 (2008) 263–267.
- [24] P.B. Hitchcock, K.R. Seddon, T. Welton, *J. Chem. Soc., Dalton Trans.* (1993) 2639–2643.
- [25] F. Zordan, G.M. Espallargas, L. Brammer, *CrystEngComm* 8 (2006) 425–431.
- [26] M. Czugler, L. Kótai, B. Sreedhar, A. Rockenbauer, I. Gács, S. Holly, *Eur. J. Inorg. Chem.* (2002) 3298–3304.
- [27] R.D. Willett, F. Awwadi, R. Butcher, *Cryst. Growth Des.* 3 (2003) 301–311.
- [28] S.N. Herringer, M.M. Turnbull, C.P. Landee, J.L. Wikaira, *J. Coord. Chem.* 62 (2009) 863–875.
- [29] C.L. Maclaurin, M.F. Richardson, *Acta Cryst.* C39 (1983) 854–856.
- [30] X. Han, D.W. Armstrong, *Acc. Chem. Res.* 40 (2007) 1079–1086.
- [31] D. Zhao, Z. Fei, T.J. Geldbach, R. Scopelliti, P.J. Dyson, *J. Am. Chem. Soc.* 126 (2004) 15876–15882.
- [32] J.D. Holbrey, M.B. Turner, W.M. Reichert, R.D. Rogers, *Green Chem.* 5 (2003) 731–736.
- [33] F. Neve, A. Crispini, *CrystEngComm* 9 (2007) 698–703.
- [34] A.C. Kathalikkattil, S. Damodaran, K.K. Bisht, E. Suresh, *J. Mol. Struct.* 985 (2011) 361–370.
- [35] A.C. Kathalikkattil, P.S. Subramanian, E. Suresh, *Inorg. Chim. Acta* 365 (2011) 363–370.
- [36] A.C. Kathalikkattil, K.K. Bisht, P.S. Subramanian, E. Suresh, *Polyhedron* 29 (2010) 1801–1809.

- [37] A.C. Kathalikkattil, P.S. Subramanian, S. Eringathodi, J. Chem. Crystallogr. 40 (2010) 1087–1093.
- [38] K.K. Bisht, A.C. Kathalikkattil, E. Suresh, Cryst. Growth Des. doi: 10.1021/cg2014094.
- [39] G.M. Sheldrick, SAINT 5.1 ed., Siemens Industrial Automation Inc., Madison, WI, 1995.
- [40] SADABS, Area Detector Absorption Correction Program, Bruker Analytical X-ray, Madison, WI, 1997.
- [41] G.M. Sheldrick, SHELXTL Reference Manual: Version 5.1, Bruker AXS, Madison, WI, 1997.
- [42] G.M. Sheldrick, SHELXL-97: Program for Crystal Structure Refinement, University of Göttingen, Göttingen, Germany, 1997.
- [43] A.L. Spek, J. Appl. Crystallogr. 36 (2003) 7–13.
- [44] P. Hrobárik, R. Reviakine, A.V. Arbuznikov, O.L. Malkina, V.G. Malkin, F.H. Köhler, M. Kaupp, J. Chem. Phys. 126 (2007) 024107-1–024107-19.
- [45] F. Rastrelli, A. Bagno, Magn. Reson. Chem. 48 (2010) S132–S141.
- [46] A.K. Brisdon, Inorganic Spectroscopic Methods, Oxford University Press Inc., New York, 2005. 30–56.
- [47] M. Gerloch, E.C. Constable, Transition Metal Chemistry, Joint publishers: VCH Verlagsgesellschaft, Federal Republic of Germany and VCH Publishers, New York, USA, 1990.
- [48] M.J. Riley, D. Neill, P.V. Bernhardt, K.A. Byriel, C.H.L. Kennard, Inorg. Chem. 37 (1998) 3635–3639.
- [49] K.E. Halvorson, C. Patterson, R.D. Willett, Acta Cryst. B46 (1990) 508–519.